Probing cilia-driven flow in living embryos using femtosecond laser ablation and fast imaging.

Willy Supatto*, Scott E. Fraser, Julien Vermot
Biological Imaging Center, California Institute of Technology,
1225 California Blvd., Pasadena, CA 91125, USA

ABSTRACT

Embryonic development strictly depends on fluid dynamics. As a consequence, understanding biological fluid dynamic is essential since it is unclear how flow affects development. For example, the specification of the left-right axis in vertebrates depends on fluid flow where beating cilia generate a directional flow necessary for breaking the embryonic symmetry in the so-called left-right organizer. To investigate flow dynamics *in vivo* proper labeling methods necessitate approaches that are compatible with both normal biology and *in vivo* imaging. In this study, we describe a strategy for labeling and analyzing microscopic fluid flows *in vivo* that meets this challenge. We developed an all-optical approach based on three steps. First we used sub-cellular femtosecond laser ablation to generate fluorescent micro-debris to label the flow. The non-linear effect used in this technique allows a high spatial confinement and a low invasiveness, thus permitting the targeting of sub-cellular regions deep inside the embryo. Then, we used fast confocal imaging and 3D-particle tracking were used to image and quantify the seeded flow. This approach was used to investigate the flow generated within zebrafish left-right organizer, a micrometer scale ciliated vesicle located deep inside the embryo and involved in breaking left-right embryonic symmetry. We mapped the velocity field within the vesicle and surrounding a single beating cilium, and showed that this method can address the dynamics of cilia-driven flows at multiple length scales. We could validate the flow features as predicted from previous simulations. Such detailed descriptions of fluid movements will be valuable in unraveling the relationships between cilia-driven flow and signal transduction. More generally, this all-optical approach opens new opportunities for investigating microscopic flow in living tissues.

Keywords: Femtosecond laser ablation, multiphoton microscopy, spinning-disk confocal microscopy, 3D-particle tracking, zebrafish, Kupffer's vesicle, cilia-driven flow.

1. INTRODUCTION

1.1 Cilia-driven flow and left-right symmetry breaking in vertebrate embryos

The analysis of cilia-driven fluid lows is becoming critical since it is increasingly recognizes that cell responses to mechanical flows are involved in major events of embryonic development and adult homeostasis [1]. Furthermore, cilia are sending key epigenetic signals during major events of embryo development, such as inner ear development [2], neuronal migration [3; 4; 5], or left-right patterning. A classical case concerns left-right axis specification in vertebrates, where the beating cilia are generating a directional flow necessary for breaking the embryonic symmetry in the so-called left-right organizer [3]. The signal transduction involved in this process remain unclear and the exact role of cilia during symmetry breaking is still debated [6]. In addition, a consensus has not yet been reached for modeling how directional flow is generated by the beating cilia [7; 8; 9; 10]. Only a few quantitative experimental data describing the process *in vivo* are available to test the different models. These data mainly describe a single system, the mouse node, but the left-right organizers display a great variety of morphology amongst vertebrates [11; 12; 13; 14]. Since cilia-generated fluid motion are pivotal in most vertebrates for left-right axis specification [15; 16], we developed an approach for probing the flow in living zebrafish embryos [17], where the left-right organizer (also called the Kupffer's vesicle, KV) is poorly described. The KV is a cavity filled with aqueous medium which is located beneath several layers of mesodermal cells in the embryonic tail bud (Fig. 1) [18; 19]. This transient organ appears at bud stage (10 hpf, hours post fertilization) and disappears after 26 somites stage (24 hpf) [20]. During this time period, the diameter of the vesicle increases from 20 to 80 μm (ie a volume of 4 to 250 pL) and goes from 70 to 120 μm below the mesodermal cell layer (Fig. 1).

*supatto@caltech.edu;

Commercial and Biomedical Applications of Ultrafast Lasers IX, edited by Joseph Neev, Stefan Nolte, Alexander Heisterkamp, Rick P. Trebino, Proc. of SPIE Vol. 7203, 72030B

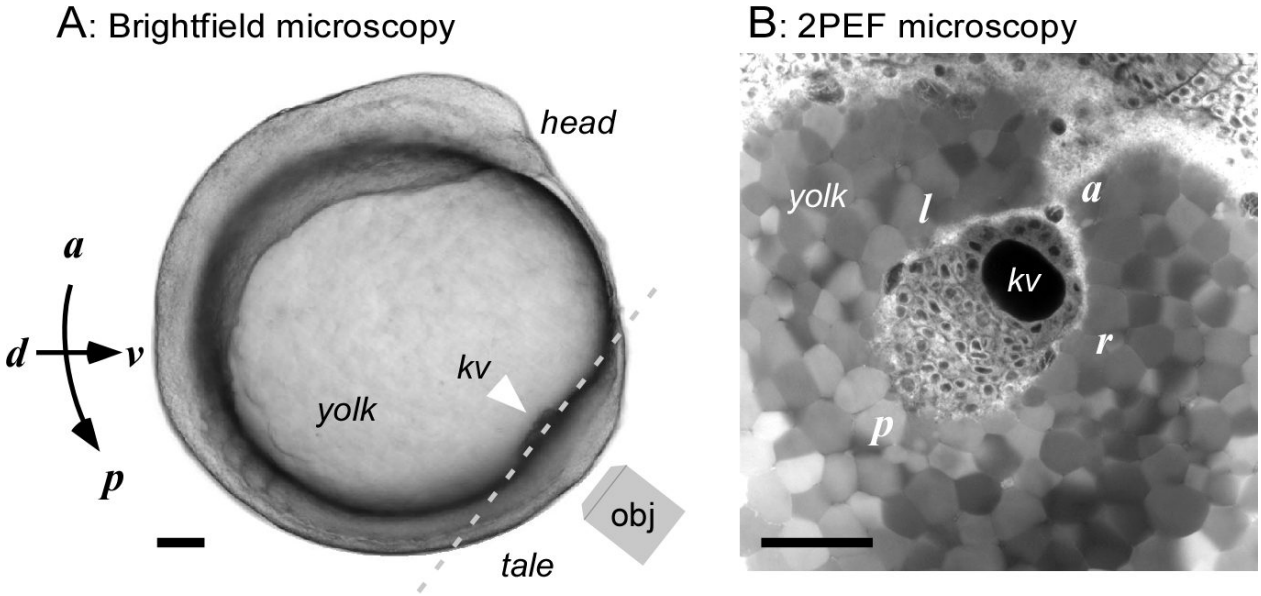

Fig. 1. The Kupffer's vesicle is the left-right organizer in zebrafish embryos. (A) Brightfield imaging of a 6-somite stage embryo (lateral view) showing the position of the KV (white arrowhead) and the position of the objective when imaged. The dashed gray line indicates the typical plane of imaging, perpendicular to the dorso-ventral axis, such as the dorsal view in (B). (B) Dorsal view of the KV using 2PEF microscopy and Bodipy TR as fluorescent labeling. ***a***: anterior, ***p***: posterior, ***d***: dorsal, ***v***: ventral, ***l***: left, ***r***: right, ***kv***: Kupffer's vesicle, **obj**: objective. Scale bar: 50 µm.

1.2 An all-optical approach to quantify microscopic fluid flow combining femtosecond laser ablation, fast imaging and 3D-particle tracking

Investigating flow dynamics *in vivo* requires the use of the appropriate procedure for flow labeling compatible with normal biology. In fluid mechanics, the standard method to analyze flows relies on seeding the fluid with tracer particles. In biology, this procedure is painful when the moving fluids are hard to access. The injection of tracer particles with a needle in a micrometer scale structure located deep inside a living organism, such as the KV, is challenging and invasive. To circumvent this limitation and minimize the possible artifacts due to experimental manipulation, we took advantage of the properties of femtosecond laser ablation [21; 22]. By allowing the disruption of cell integrity with extreme spatial confinement and low collateral damages, this technique has first been used to perform nanometer-scale dissections in thin specimen [23; 24]. Furthermore, thanks to the use of near-infrared radiations allowing a deep penetration inside thicker specimen, it has been applied in neuroscience [25; 26], and developmental biology [27; 28; 29]. Using this technique, we devised the following all-optical strategy to label, image and quantify the flow *in vivo* within the KV (Fig. 2). After labeling the KV cells with a fluorecent dye (Fig. 2A-B), sub-cellular femtosecond laser ablation is used to target a single cell lining the cavity and generate a slit in the cytoplasmic membrane (Fig. 2C). The resulting optical disruption induced the release of fluorescently labeled cell debris inside the vesicle, subsequently seeding the flow with fluorescent particles (Fig. 2D). Subsequent fast 4D-confocal imaging [30] and 3D-particle tracking are used to image and quantify the seeded flow. We illustrate this approach by characterizing the flow generated within the KV and surrounding a single beating cilium.

2. MATERIAL AND METHODS

Zebrafish embryos were loaded with Bodipy TR dye (Molecular Probe) for 30 minutes and mounted in agarose 0.7% in Danieau solution (Bodipy TR labeling in gray in Fig. 1B, 3A, and 4). This dye permeates cell membranes and selectively stains mitochondria and endomembranous organelles such as endoplasmic reticulum and the Golgi apparatus. 2-photon excited fluorescence (2PEF) microscopy (Fig. 1B and Fig. 3) and femtosecond laser ablation were performed at 820nm using a Chameleon Ultra laser and a Zeiss LSM510 microscope on 6 somite-stage embryos. Green and red channels

(Fig. 3) correspond to 500-550nm and 575-640nm band-pass filtering of the emmited light, respectively. The typical conditions for deep tissue ablation were: 5µm linescan, 200µm/s scan speed (512 pixel line with 50 µs pixel dwell time), 300fs pulses, 80MHz repetition rate, 820nm wavelength, using an average power of 250 to 300mW after the objective. Fast confocal images (Fig 4) were collected on a Perkin-Elmer Spinning-disk confocal (SDC) microscope. The acquisition parameters were: 44 frames per second, 11 z-planes every 1µm, 0.4µm per pixel in x and y (corresponding to 3D stacks at 4Hz). Experiments were done using a 40x/NA 1.1 objective lens (Zeiss). 3D-particle tracking was performed automatically with Imaris (Bitplane) and manually corrected. The velocity field analysis was done with custom Matlab scripts. The vesicle surface and the cilium volume (Fig. 6) were manually segmented from experimental data.

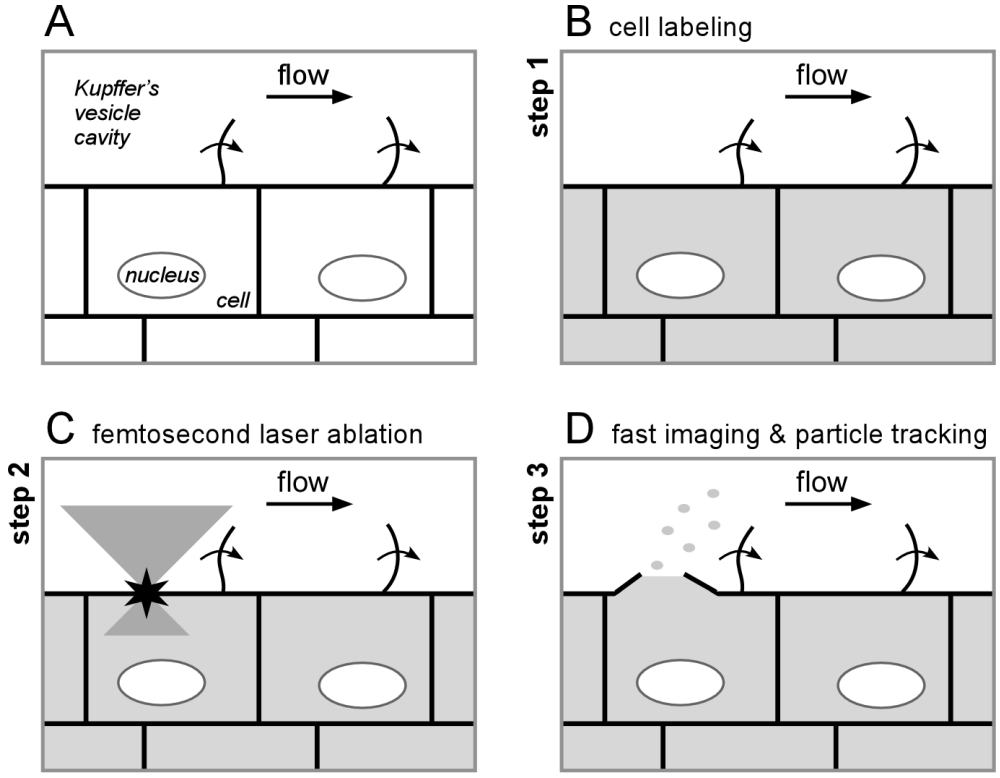

Fig. 2. All optical strategy to label, image and quantify the flow generated within the Kupffer's vesicle. The cells of the HV (A) are first labeled with a dye (B). The femtoseconf laser ablation is used to targed the membrane of a single cell a the surface of the cavity (C) and generate fluorrescent particles that seed the flow (D).

3. RESULTS

3.1 Femtosecond laser ablation in zebrafish embryos

The minimal spatial extension of femtosecond laser ablation in tissues increases with depth and depends on the tissue optical properties. We first characterized the optical properties of the embryonic tissue by measuring a phenomenological 2PEF attenuation length (L) of the excitation light at 820nm. Experimentally, it is observed that the 2PEF signal detected in thick samples decreases exponentially with depth as $\exp(-z/L)$ for a constant incident power at the tissue surface, where z is the imaging depth. Under the assumptions that absorption can be neglected and that fluorescence collection efficiency is constant with depth, L characterizes the excitation light scattering and the optical aberrations due to the tissue. Furthermore, if the optical aberrations can be neglected, L is half of the scattering length of the excitation light in the tissue [31]. We found that L~70µm in the tissue surrounding the Kupffer vesicle in 6 somite stage zebrafish embryos (N=4). Then, we investigated the ablation depth where a sub-cellular 3D-confinement was still

achievable when focusing femtosecond laser pulses deep inside the embryo. Femtosecond pulse trains (300fs, 820nm, 80 MHz) were focused (1.1 NA objective) on mesodermal cells, 70 μm beneath the epidermal cell layer of live embryos. The effect of each ablation was observed after attenuating the laser power and recording the 2-photon excited fluorescence (2PEF) images of the endogenous fluorescence around the targeted area (Fig. 3). Successful ablations were defined by the generation of intense broadband fluorescence in the targeted region recorded in the green channel (Fig. 3B, as described in [27]). A sub-cellular spot (~20 fL) was observed resulting from the energy deposited by the laser pulses, thereby delimiting the ablation volume. No visible damages were detected between the focal volume and the surface of the embryo (Fig. 3) demonstrating the 3D confinement of the ablation at this depth. Thus, the sub-cellular micrometer-scale ablation was achievable down to a depth comparable to *L*.

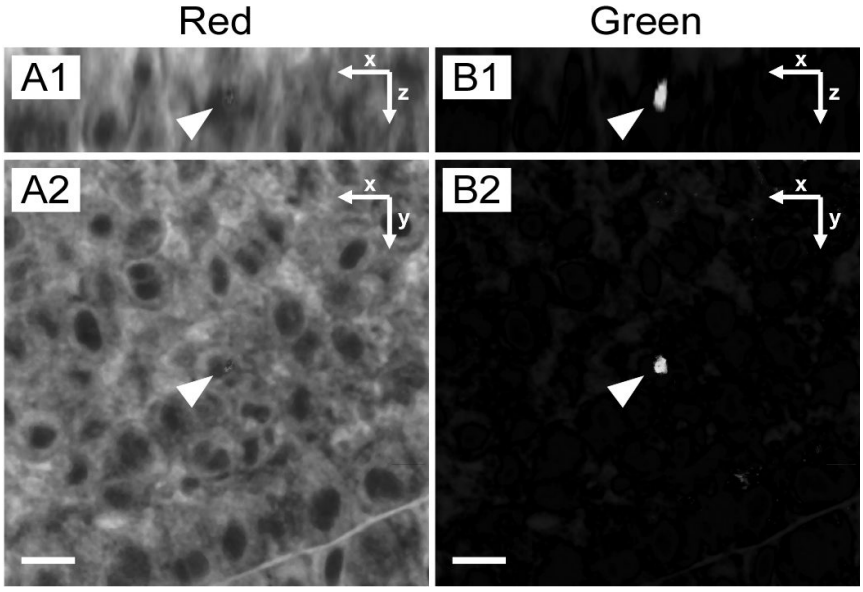

Fig. 3. 3D-confined ablation inside the zebrafish tale bud. Red (A) fluorescent signal after ablation inside an dye labeled embryo. The green fluorescence is generated as a result of the laser ablation (B).. Two views, in x-z (A1, B1) and in x-y (A2, B2), showing the 3D confinement of the ablation (Green, <5 μm in each direction) generated 70 μm deep inside the embryo. Scale bar: 10 μm.

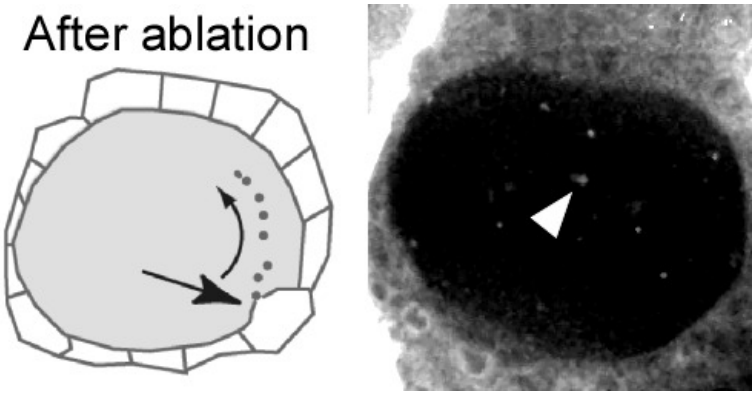

Fig. 4. Flow seeding by fluorescent particles after laser ablation. Fast confocal microscopy allows imaging of the fluorescent microdebris (white arrowhead) seeding the flow.

We took advantage of the 3D confinement of femtosecond-induced ablations to generate a slit in the cytoplasmic membrane of a single cell lining the cavity (N=20, data not shown). The resulting optical disruption induced the release of fluorescently labeled cell debris inside the vesicle, subsequently seeding the flow with fluorescent particles (Fig. 4). We evaluated the invasiveness of this approach by looking at the vesicle morphology after ablation and by checking left-right axis specification in the manipulated embryos. We found that the vesicle morphology remained the same after ablation (Fig. 4) and no left-right defects were observed (N=8).

3.2 Fast imaging and quantification of the fluid flow generated within the Kupffer's vesicle

The seeding of the fluid with fluorescent particles allowed us to investigate the three-dimensional motion of the flow within the KV. The motion of the particles trapped in the flow was too fast to be imaged with 2PEF microscopy. Therefore, the particles were imaged in 3D after ablation using a fast confocal microscope at 44 frames per second (4 z-stack per second) and 3D-tracked using image processing. The particles located 10 µm away from the vesicle surface exhibited a circular motion following a counterclockwise rotation (dorsal view) around the dorso-ventral axis as shown in Fig. 5B (experimental dat not shown) confirming previous observations on the KV [18; 19]. The time-independent feature of this flow during the observation period was demonstrated by building an overlay of the different particle tracks recorded at various time windows on a same image (data not shown). The maximum observed speeds typically ranged from 10 to 50 $\mu m.s^{-1}$, leading the particles to perform a full vesicle revolution every 15 seconds. Assuming that the viscosity within the vesicle is close to the viscosity of pure water, the corresponding Reynolds number is of the order of 10^{-3}.

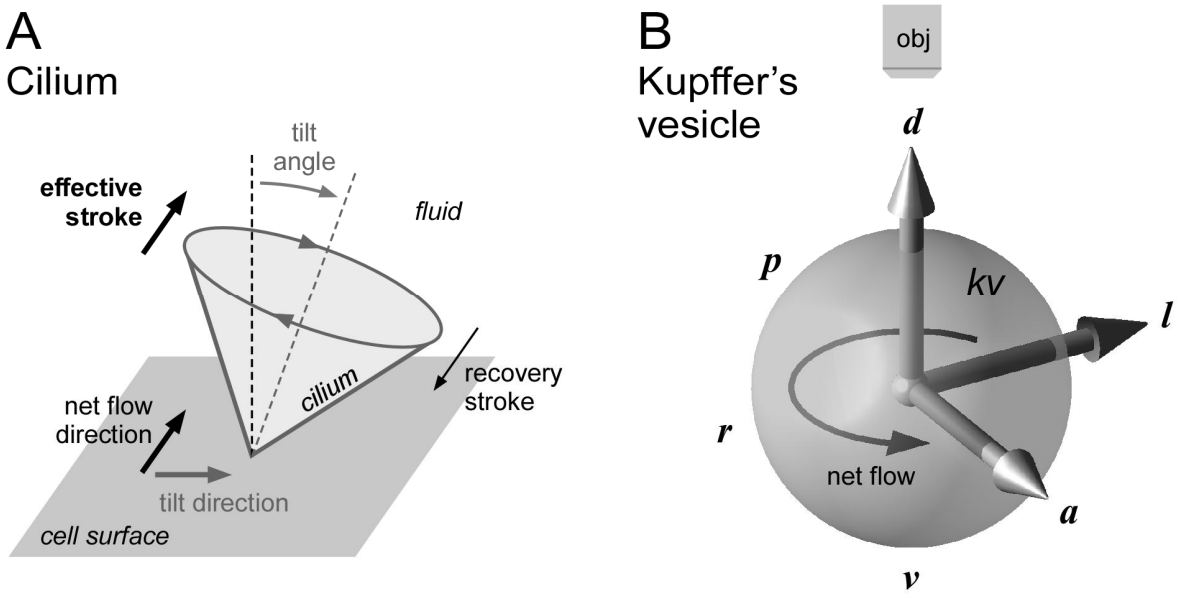

Fig. 5. Flow generation within the Kupffer's vesicle. The clockwise rotation of the cilium (A) around an tilited axis generates an effective and a recovery stroke, leading to a net flow in a direction perpenicular to the tilt direction. The directional flow generated within the KV (B) exhibits a counterclockwise rotation when image from the dorsal side. ***a***: anterior, ***p***: posterior, ***d***: dorsal, ***v***: ventral, ***l***: left, ***r***: right, ***kv***: Kupffer's vesicle, **obj**: objective.

3.3 Quantifying the fluid flow surrounding a single beating cilium *in vivo*

Understanding how the directional flow is generated within the KV requires the characterization of the spatial position, the direction of rotation and the tilt of the beating cilia. Yet, the direct fluorescence imaging in 3D of these cilia is challenging because they beat fast (~25 Hz) and are localized deep below the tissue surface. Fortunately, the particles traveling near the envelope of a beating cilium can be trapped into a vortical flow with the same rotation direction, but with a significantly slower speed, as predicted by Smith *et al.* simulation [32]. As a consequence, we projected that fast confocal microscopy would allow to image the trajectories of these particles and indirectly probe the cilium

characteristics. Indeed, particles trapped into vortical flows were observed close to the cell surface (see position within the KV in Fig. 6A2) and allowed to localize a potential beating cilium. Particle tracking and reconstruction of the velocity field in 3D (Fig. 6A1) revealed a transition between the directional flow (>10µm) and the vortical flow closer to the surface (<10µm). The presence of chaotic advection generated around the envelope of the cilium was observed by following the quick divergence of nearby tracks (data not shown). In the context of laminar flow at low Reynolds number, this chaotic behavior is an original characteristic predicted by previous simulations [32]. Together, these features demonstrate the presence of a cilium in the observed area.

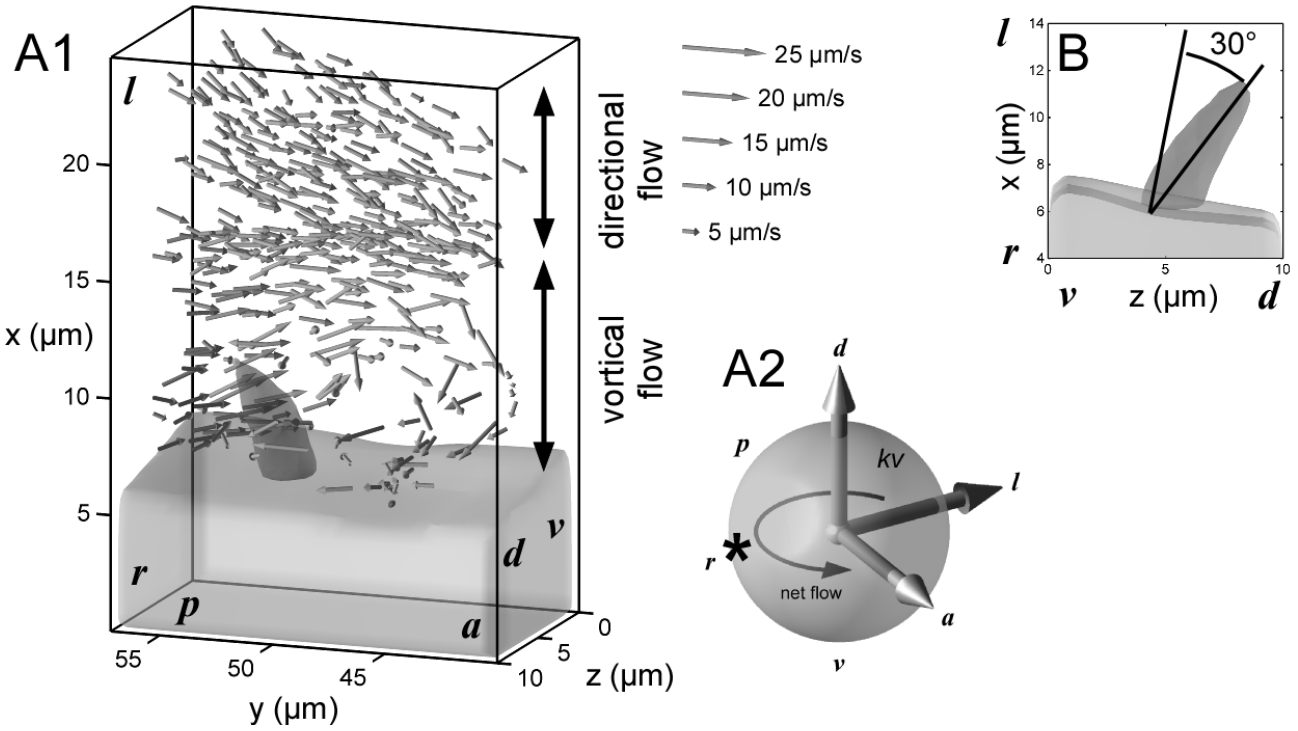

Fig. 6. Velocity map a the flow surrounding a single beating cilium *in vivo*. The 3D-tracking of particles close to the surface of the KV (see asterisk in A2) allows measure the velocity field surrounding a single beating cilium (A1). The voulume where no particles are observed (dark gray in A1 and B) allows to determine the tilt of the rotation axis of the cilium (B). ***a***: anterior, ***p***: posterior, ***d***: dorsal, ***v***: ventral, ***l***: left, ***r***: right, ***kv***: Kupffer's vesicle. Light gray surface in A1 and B: surface of the KV cells.

A directional flow motion can be driven by cilia with a beating axis tilted in a plane perpendicular to the flow [7; 13; 33] as shown in Fig 5A. To define the rotation axis of the observed cilium, we identified the main direction of a volume around which the particles spin. Its surface was manually reconstructed by drawing the envelope of the space where no particle was detected (dark gray surface in Fig. 6). The axis exhibits a 30 degree angle tilt towards the dorsal direction (Fig. 6B). This angle is close to the 35 degree value anticipated by simulations to generate the optimal advection [10]. Considering the position of the cilium and the direction of the net flow measured inside the vesicle (Fig. 5B), the dorsal tilt is in accordance with the theoretical model [7]. Furthermore, the clockwise rotation (view from the tip of the cilium) of the trapped particles gives the rotation direction of the cilium and corroborates previous observations [13; 33]. The good agreement between our experimental observations and the features recently predicted by numerical simulations confirms that this approach can reveal several characteristics of a cilium and the surrounding flow. It also validates the non-invasiveness of this approach. Ultimately, a detailed description of cilia-driven fluid movements is expected to be valuable in unraveling the relationship between flow and signal transduction that are crucial for maintaining the asymmetry of the embryo.

4. CONCLUSION

The experimental quantification of biological fluid dynamics *in vivo* and at the micrometer scale is technically challenging. As a consequence, the contribution of fluid mechanics generated by cilia to biology remains poorly understood. Here we describe an all-optical strategy to label and quantify biological flows *in vivo* by combining highly localized femtosecond laser ablation, fast confocal imaging and 3D-particle tracking. This strategy permits to map the flow patterns at multiple scales (ranging from sub-cellular to multi-cellular scales) and should be applicable in biological systems that are of challenging access. Most importantly, the invasiveness of the procedure is minimal and maintains the necessary environment for *in vivo* imaging at the cilium scale. The observed flow surrounding a beating cilium within the Kupffer vesicle exhibits the same features as predicted by numerical simulations, validating the outcome of our mapping strategy. Ultimately, a detailed description of cilia-driven fluid movements is expected to be valuable in unraveling the relationship between flow and signal transduction that are crucial for maintaining the asymmetry of the embryo. This approach also opens new opportunities for investigating the cilia dynamics in living tissues.

ACKNOWLEDGMENTS

We are grateful to D. Wu and T. Truong for critical comments, the Caltech Biological Imaging Center, and P. Bjo¨rkman for sharing equipments. J.V. was supported by the Human Frontier Science Program Fellowship. W.S. was supported by a Caltech Biology Division Fellowship. This work was supported by the Biological Imaging Center of the Caltech Beckman Institute and a Centers of Excellence in Genomic Sciences grant from the National Institutes of Health (P50 HG004071).

REFERENCES

[1] Cartwright J. H. E., Piro O., and Tuval I., "Fluid dynamics in developmental biology: moving fluids that shape ontogeny," HFSP Journal, Adv. Online Pub. (2009).

[2] Colantonio J. R., Vermot J., Wu D., Langenbacher A. D., Fraser S., Chen J. N., and Hill K. L., "The dynein regulatory complex is required for ciliary motility and otolith biogenesis in the inner ear," Nature 457(7226), 205-209 (2009).

[3] Hirokawa N., Tanaka Y., Okada Y., and Takeda S., "Nodal flow and the generation of left-right asymmetry," Cell 125(1), 33-45 (2006).

[4] Riley B. B., Zhu C. W., Janetopoulos C., and Aufderheide K. J., "A critical period of ear development controlled by distinct populations of ciliated cells in the zebrafish," Developmental Biology 191(2), 191-201 (1997).

[5] Sawamoto K., Wichterle H., Gonzalez-Perez O., Cholfin J. A., Yamada M., Spassky N., Murcia N. S., Garcia-Verdugo J. M., Marin O., Rubenstein J. L. R., Tessier-Lavigne M., Okano H., and Alvarez-Buylla A., "New neurons follow the flow of cerebrospinal fluid in the adult brain," Science 311(5761), 629-632 (2006).

[6] Tabin C., "Do we know anything about how left–right asymmetry is first established in the vertebrate embryo?," Journal of Molecular Histology 36, 317-323 (2005).

[7] Cartwright J. H. E., Piro O., and Tuval I., "Fluid-dynamical basis of the embryonic development of left-right asymmetry in vertebrates," Proc Natl Acad Sci U S A 101(19), 7234-7239 (2004).

[8] Vilfan A., and Julicher F., "Hydrodynamic flow patterns and synchronization of beating cilia," Physical Review Letters 96(5), 058102 (2006).

[9] Buceta J., Ibanes M., Rasskin-Gutman D., Okada Y., Hirokawa N., and Izpisua-Belmonte J. C., "Nodal cilia dynamics and the specification of the left/right axis in early vertebrate embryo development," Biophysical Journal 89(4), 2199-2209 (2005).

[10] Smith D. J., Blake J. R., and Gaffney E. A., "Fluid mechanics of nodal flow due to embryonic primary cilia," Journal of the Royal Society Interface 5(22), 567-573 (2008).

[11] Blum M., Andre P., Muders K., Schweickert A., Fischer A., Bitzer E., Bogusch S., Beyer T., van Straaten H. W. M., and Viebahn C., "Ciliation and gene expression distinguish between node and posterior notochord in the mammalian embryo," Differentiation 75(2), 133-146 (2007).

[12] Essner J. J., Vogan K. J., Wagner M. K., Tabin C. J., Yost H. J., and Brueckner M., "Conserved function for embryonic nodal cilia," Nature 418(6893), 37-38 (2002).

[13] Okada Y., Takeda S., Tanaka Y., Belmonte J. C. I., and Hirokawa N., "Mechanism of nodal flow: A conserved symmetry breaking event in left-right axis determination," Cell 121(4), 633-644 (2005).
[14] Schweickert A., Weber T., Beyer T., Vick P., Bogusch S., Feistel K., and Blum M., "Cilia-driven leftward flow determines laterality in Xenopus," Current Biology 17(1), 60-66 (2007).
[15] Levin M., "Left-right asymmetry in embryonic development: a comprehensive review," Mechanisms of Development 122(1), 3-25 (2005).
[16] Speder P., Petzoldt A., Suzanne M., and Noselli S., "Strategies to establish left/right asymmetry in vertebrates and invertebrates," Current Opinion in Genetics & Development 17(4), 351-358 (2007).
[17] Supatto W., Fraser S. E., and Vermot J., "An all-optical approach for probing microscopic flows in living embryos," Biophysical Journal 95(4), L29-L31 (2008).
[18] Essner J. J., Amack J. D., Nyholm M. K., Harris E. B., and Yost J., "Kupffer's vesicle is a ciliated organ of asymmetry in the zebrafish embryo that initiates left-right development of the brain, heart and gut," Development 132(6), 1247-1260 (2005).
[19] Kramer-Zucker A. G., Olale F., Haycraft C. J., Yoder B. K., Schier A. F., and Drummond I. A., "Cilia-driven fluid flow in the zebrafish pronephros, brain and Kupffer's vesicle is required for normal organogenesis," Development 132(8), 1907-1921 (2005).
[20] Cooper M. S., and Damico L. A., "A cluster of noninvoluting endocytic cells at the margin of the zebrafish blastoderm marks the site of embryonic shield formation," Developmental Biology 180(1), 184-198 (1996).
[21] Vogel A., Noack J., Huttman G., and Paltauf G., "Mechanisms of femtosecond laser nanosurgery of cells and tissues," Applied Physics B 81(8), 1015-1047 (2005).
[22] Kohli V., and Elezzabi A. Y., "Prospects and developments in cell and embryo laser nanosurgery," Wiley Interdisciplinary Reviews: Nanomedicine and Nanobiotechnology 1(1), 11-25 (2009).
[23] Tirlapur U. K., and König K., "Cell biology: Targeted transfection by femtosecond laser," Nature 418, 290-291 (2002).
[24] Kumar S., Maxwell I. Z., Heisterkamp A., Polte T. R., Lele T. P., Salanga M., Mazur E., and Ingber D. E., "Viscoelastic retraction of single living stress fibers and its impact on cell shape, cytoskeletal organization, and extracellular matrix mechanics," Biophysical Journal 90(10), 3762-3773 (2006).
[25] Yanik M. F., Cinar H., Cinar H. N., Chisholm A. D., Jin Y., and Ben-Yakar A., "Neurosurgery: Functional regeneration after laser axotomy," Nature 432(7019), 822 (2004).
[26] Nishimura N., Schaffer C. B., Friedman B., Tsai P. S., Lyden P. D., and Kleinfeld D., "Targeted insult to subsurface cortical blood vessels using ultrashort laser pulses: three models of stroke," Nature Methods 3(2), 99-108 (2006).
[27] Supatto W., Debarre D., Moulia B., Brouzes E., Martin J. L., Farge E., and Beaurepaire E., "In vivo modulation of morphogenetic movements in Drosophila embryos with femtosecond laser pulses," Proc. Natl. Acad. Sci. U. S. A. 102(4), 1047-1052 (2005).
[28] Supatto W., Débarre D., Farge E., and Beaurepaire E., "Femtosecond pulse-induced microprocessing of live Drosophila embryos," Medical Laser Application 20(30), 207-216 (2005).
[29] Desprat N., Supatto W., Pouille P. A., Beaurepaire E., and Farge E., "Tissue deformation modulates twist expression to determine anterior midgut differentiation in Drosophila embryos," Developmental Cell 15(3), 470-477 (2008).
[30] Vermot J., Fraser S., and Liebling M., "Fast fluorescence microscopy for imaging the dynamics of embryonic development," HFSP Journal 2(3), 143-155 (2008).
[31] Oheim M., Beaurepaire E., Chaigneau E., Mertz J., and Charpak S., "Two-photon microscopy in brain tissue: parameters influencing the imaging depth," Journal of Neurosciences Methods 111, 29-37 (2001).
[32] Smith D. J., Gaffney E. A., and Blake J. R., "Discrete cilia modeling with singularity distributions: Application to the embryonic node and the airway surface liquid," Bulletin of Mathematical Biology 69(5), 1477-1510 (2007).
[33] Nonaka S., Yoshiba S., Watanabe D., Ikeuchi S., Goto T., Marshall W. F., and Hamada H., "De novo formation of left-right asymmetry by posterior tilt of nodal cilia," PLoS Biology 3(8), 1467-1472 (2005).